ACS Macro Letters

pubs.acs.org/macroletters Letter

Unlocking Ring-Opening Polymerization of Glycidyl Propargyl Ether via Lewis Pair Organocatalysts

Byungwoo Yoo,[†] Jinsu Baek,[†] and Byeong-Su Kim*

Cite This: ACS Macro Lett. 2025, 14, 1344−1351 Read Online

ACCESS | Metrics & More | Article Recommendations | Supporting Information

ABSTRACT: Alkyne groups provide exceptional versatility for functionalization in macromolecular systems. However, the controlled anionic ring-opening polymerization (AROP) of epoxide monomers bearing terminal alkynes remains challenging due to the lability of alkynes under strongly basic conditions. Herein, we present a controlled AROP of glycidyl propargyl ether enabled by Lewis pair organocatalysis, employing a phosphazene base and triethylborane. This catalytic system suppresses undesired interactions with the acidic alkyne proton, allowing precise control over the polymerization degree (25−100) with narrow dispersity ($Đ$ < 1.1) and high initiation efficiency in the synthesis of poly(glycidyl propargyl ether). Moreover, this method yields diverse polymer architectures, including diblock copolymers via atom transfer radical polymerization and triblock copolymers using a macroinitiator strategy. Post-polymerization modification is demonstrated through Cu-catalyzed azide−alkyne cycloaddition and thiol−yne reactions. We envision that this approach significantly broadens access to alkyne-functionalized AROP systems and paves the way for their use in diverse applications.

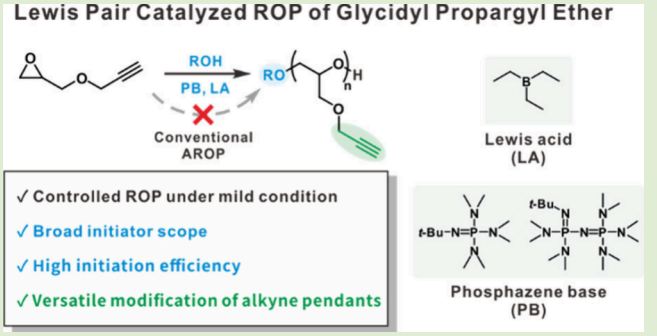

Alkyne groups are highly valued in chemistry for their high reactivity and broad applicability in organic synthesis, which encompasses diverse addition and coupling reactions.[1,2] Owing to their chemo- and regioselective behavior, these functionalities readily participate in transformations, such as the Cu(I)-catalyzed azide−alkyne cycloaddition (CuAAC), under mild conditions, affording it a crucial component for bioconjugation strategies. Moreover, such reactivity is particularly advantageous in polymer chemistry, where simultaneous and orthogonal control over multiple functional groups is essential for achieving well-defined polymer structures and desirable properties. Reflecting this versatility, numerous studies have demonstrated the utility of alkynes in polymer synthesis, particularly in topology control,[3−6] side-chain modification,[7] block copolymer fabrication,[8] and network formation.[9] Beyond CuAAC, several other strategies have also been proposed for utilizing alkyne groups in polymer systems, including the thiol−yne reaction[10] and alkyne−metal coordination.[11]

Glycidyl propargyl ether (GPE) serves as a versatile monomer for functional polyether synthesis, owing to its alkyne functionality. Notably, polyethers, such as poly(ethylene oxide) (PEO), are widely utilized in biomedical applications, drug delivery systems, and functional materials owing to their high hydrophilicity and biocompatibility. Given these advantages, incorporating GPE into polyether synthesis offers synergistic benefits by leveraging the reactivity of alkynes for orthogonal modifications. Despite its applicability, GPE is not amenable to conventional anionic ring-opening polymerization (AROP) due to the intrinsic acidity of the terminal alkyne under strongly basic conditions.

To overcome this limitation, several studies have investigated an alternative approach of employing monomer-activated ring-opening polymerization (MAROP) for the synthesis of alkyne-functionalized polyethers.[7,12,13] Unlike conventional AROP, MAROP involves the introduction of a strong Lewis acid, such as triisobutylaluminum, which interacts with the oxirane moiety in the monomer, enhancing its susceptibility to nucleophilic attack.[14−17] This approach enables polymerization without strong bases, thereby reducing the overall basicity of the reaction medium and facilitating the polymerization of GPE. Although base-free conditions offer a milder environment, they often fail to activate initiators commonly employed in conventional AROP, thus limiting the range of suitable initiators.[18] Moreover, studies have shown that MAROP exhibits low initiation efficiency, making chain-end modification challenging.[19] As a result, the diversity of accessible polymer structures is substantially limited. There-

Received: July 26, 2025
Revised: September 1, 2025
Accepted: September 2, 2025
Published: September 5, 2025

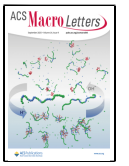

Scheme 1. (a) Previous Approaches for the Polymerization of GPE, (b) This Work: Lewis Pair-Catalyzed Ring-Opening Polymerization of GPE Using Various Initiators for the Synthesis of PGPE, and (c) Synthetic Pathways toward PGPE-Based Block Copolymers

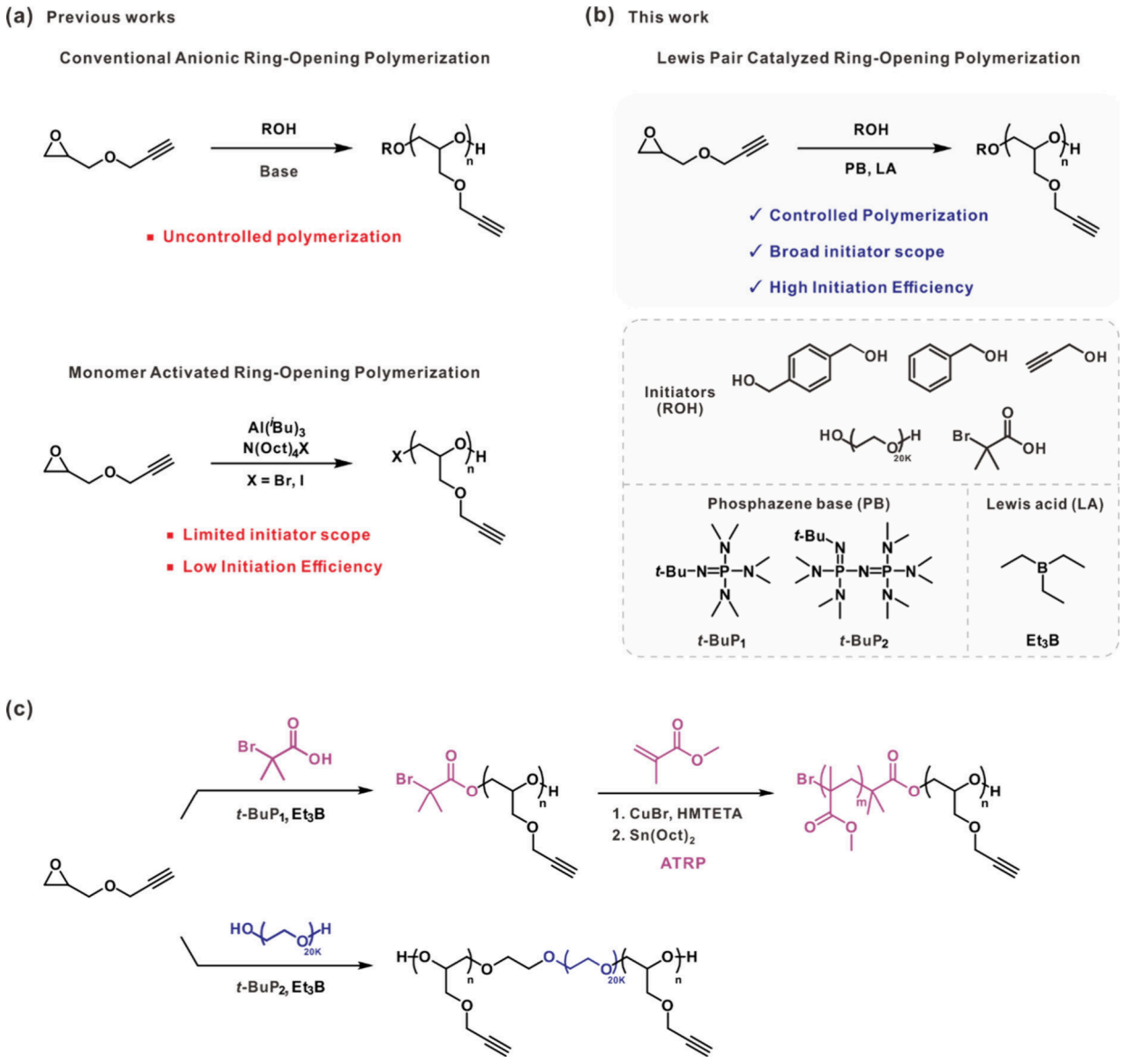

fore, it is still highly desirable to develop controlled methods to polymerize GPE with predictable polymer architectures and defined chain-end groups while preserving the alkyne moiety for further modifications.

To this end, we herein report a controlled ROP of GPE catalyzed by a Lewis pair comprising a phosphazene base and triethylborane (TEB) (Scheme 1). This system involves the activation of the initiator by a milder phosphazene base to generate a nucleophilic species, while Lewis acidic TEB coordinates to the epoxide monomer, enhancing its electrophilicity and stabilizing the anionic chain end.[20] This dual activation mechanism not only facilitates efficient polymerization but also suppresses side reactions involving base-sensitive functional groups.[21] In this context, the Zhao group has recently reported the controlled polymerization of silyl glycidyl ether under Lewis pair catalysis, successfully suppressing silyl ether exchange, a known side reaction that inhibits ROP.[22] We integrated the Lewis pair catalytic system into GPE polymerization, effectively mitigating the influence of the terminal alkyne acidity. Consequently, poly(glycidyl propargyl ether)s (PGPEs) with varying degrees of polymerization were synthesized in a controlled manner using a broad range of initiators, including 1,4-benzenedimethanol, propargyl alcohol, 2-bromoisobutyric acid, and poly(ethylene oxide). This enabled precise control over PGPE chain-end functionalities and facilitated the use of macroinitiators, thereby offering a new route toward a new type of polymer architecture. Specifically, bromo-terminated PGPE was employed to synthesize a poly(methyl methacrylate)-*b*-poly(glycidyl propargyl ether) (PMMA-*b*-PGPE) diblock copolymer via sequential atom transfer radical polymerization (ATRP), while the macroinitiator approach enabled the formation of a PGPE-*b*-PEO-*b*-PGPE triblock copolymer. Furthermore, post-polymerization modifications using CuAAC and thiol−yne reactions demonstrated the potential for functional diversification.

https://doi.org/10.1021/acsmacrolett.5c00486
ACS Macro Lett. 2025, 14, 1344−1351

Table 1. Lewis Pair Polymerization of GPE Using BDM as the Initiator[a]

entry	base (B)	reaction conditions [GPE]/[BDM]/[B]/[TEB]	target DP	conversion[b]	$M_{n,th}$[c] (kDa)	$M_{n,NMR}$[d] (kDa)	$M_{n,GPC}$[e] (kDa)	$Đ$[e]
1	*t*-BuP$_4$	25/1/0.5/0	25	>99	2.9		2.4	2.32
2	*t*-BuP$_1$	25/1/0.5/0	25	0				
3	*t*-BuP$_1$	25/1/0.5/1.5	25	93	2.7	2.7	2.5	1.06
4	*t*-BuP$_1$	50/1/0.5/1.5	50	77	4.4	3.7	3.2	1.05
5	*t*-BuP$_1$	25/0.5/0.5/1.5	50	94	5.4	6.2	4.9	1.11
6	*t*-BuP$_1$	25/0.5/0.25/1.5	50	88	5.1	5.1	4.0	1.09
7	*t*-BuP$_1$	25/0.5/0.5/1.0	50	94	5.4	6.3	5.4	1.10
8	*t*-BuP$_1$	25/0.25/0.25/1.5	100	91	10.3	10.0	7.7	1.16
9	*t*-BuP$_1$	25/0.25/0.25/0.5	100	80	9.1	11.6	8.3	1.08
10	*t*-BuP$_1$	25/0.167/0.167/0.33	150	24	4.0	5.8	3.8	1.09
11	*t*-BuP$_2$	25/0.167/0.167/0.33	150	80	13.6	14.3	11.1	1.13
12	*t*-BuP$_2$	25/0.125/0.125/0.25	200	81	18.3	15.4	12.6	1.10

[a]All reactions were conducted in bulk at room temperature. [b]Calculated from the ^{1}H NMR spectrum of the crude sample. [c]Calculated from the target monomer-to-initiator feed ratio and conversion obtained from the ^{1}H NMR spectrum of the crude sample. [d]Calculated from the ^{1}H NMR spectrum of purified PGPE. [e]Determined through GPC analysis (THF eluent, RI signal, and PEO standard).

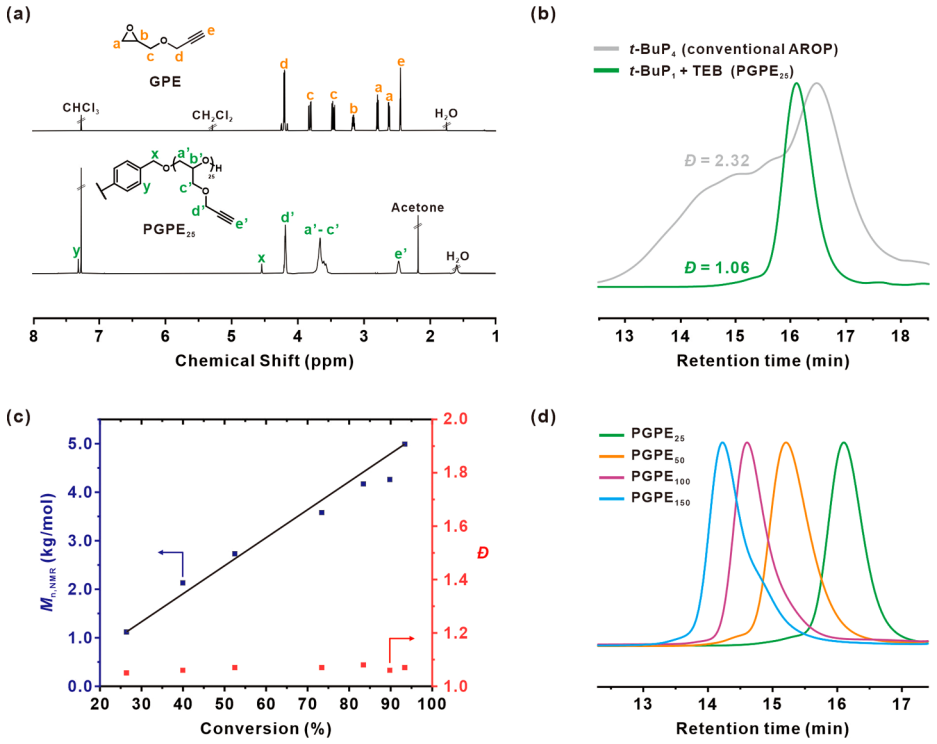

Figure 1. (a) ^{1}H NMR spectra of the (top) GPE monomer and (bottom) PGPE25 homopolymer (entry 3 in Table 1), (b) GPC traces of PGPE synthesized via (gray line) conventional AROP and (green line) *t*-BuP$_1$/TEB-catalyzed ROP, (c) evolution of $M_{n,NMR}$ and molecular weight dispersity ($Đ$) as a function of monomer conversion, and (d) GPC traces of PGPEs with the target degree of polymerization (DP) ranging from 25 to 150 (THF eluent, RI signal, and PEO standard).

The alkyne-functionalized epoxide monomer GPE was synthesized through a one-step reaction and subsequently purified by fractional distillation in a high yield (Figures S1−S3 of the Supporting Information). To evaluate the susceptibility of the alkyne moiety in GPE to basic conditions, conventional AROP was first performed in bulk using the strong phosphazene base *t*-BuP$_4$ and 1,4-benzenedimethanol (BDM) as the initiator at room temperature (entry 1 in Table 1). Although complete consumption of the epoxide was confirmed by ^{1}H NMR spectroscopy (Figure S4a), the molecular weight dispersity ($Đ$), as determined by gel permeation chromatography (GPC), was 2.32 (Figure 1b). This value is considerably higher than those typically observed for polymers synthesized via AROP, indicating that uncontrolled reactions occurred at the terminal alkyne under highly basic conditions.

Further, when the milder base *t*-BuP$_1$ was used alone, no polymerization occurred (entry 2 in Table 1 and Figure S4b). Conversely, controlled polymerization of GPE was achieved using a Lewis pair catalyst composed of *t*-BuP$_1$ and TEB. The conversion of monomer to polymer was determined by the disappearance of the epoxide peak at 3.15 ppm and the appearance of signals corresponding to the polyether backbone of PGPE at 3.49−3.79 ppm in the ^{1}H NMR spectra (Figure 1a). The resulting PGPE was further characterized by GPC and ^{13}C NMR analyses (Figure 1b and Figure S5). Notably, the GPC trace displayed a considerably narrower molecular weight dispersity ($Đ$ = 1.05) than that observed under

https://doi.org/10.1021/acsmacrolett.5c00486
ACS Macro Lett. 2025, 14, 1344−1351

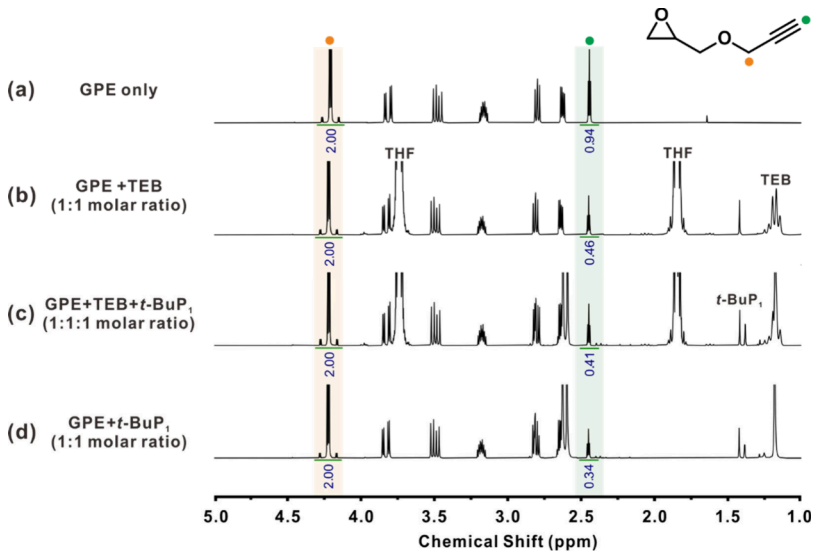

Figure 2. ^{1}H NMR spectra of (a) neat GPE monomer, (b) equimolar mixture of GPE and TEB, (c) GPE with TEB and *t*-BuP$_1$, and (d) GPE with *t*-BuP$_1$. The propargylic (orange) and terminal alkyne (green) regions are highlighted, along with their corresponding integral values.

conventional AROP conditions. In addition, to evaluate the polymerization kinetics of PGPE$_{50}$, samples collected at different reaction times were subjected to ^{1}H NMR and GPC analyses (Figure S6). As the reaction proceeded, the GPC traces exhibited a continuous shift toward a lower retention time, indicating controlled chain growth throughout polymerization. This behavior was further corroborated by the linear increase in molecular weight ($M_{n,NMR}$ and $M_{n,GPC}$) with monomer conversion while maintaining a low molecular weight dispersity during the polymerization (Figure 1c and Figure S6c).

To synthesize PGPEs with a higher DP of 50, we initially doubled the monomer feed while maintaining the molar ratio of the initiator, *t*-BuP$_1$, and the TEB constant (i.e., [GPE]/[BDM]/[*t*-BuP$_1$]/[TEB] = 50/1/0.5/1.5). However, this approach led to a reduced GPE conversion of 77%, and the number-average molecular weight (M_n) determined by both ^{1}H NMR spectroscopy and GPC was considerably lower than the target value (entry 4 in Table 1). To address this limitation, we adopted an alternative strategy wherein the molar ratio of the monomer and Lewis pair catalysts was held constant, while the initiator concentration was reduced to tune the DP of PGPE (entry 5 in Table 1). Notably, this adjustment resulted in an increased conversion of 94%, accompanied by a higher molecular weight. These results suggest that the molar ratio of monomer to catalyst is a key parameter influencing polymerization efficiency, owing to interactions between the terminal alkyne and the Lewis pair catalysts.

Based on these observations, we further examined the effect of the base-to-acid ratio (i.e., [B]/[TEB]) on the polymerization process. Notably, halving the amount of base while keeping other components constant led to a slight decrease in both conversion and molecular weight (entry 6 in Table 1). Meanwhile, reducing the amount of acid had no effect on monomer conversion but resulted in an increase in $M_{n,GPC}$ (entry 7 in Table 1). This trend became more pronounced at higher target DPs. For instance, at a target DP of 100, a base-to-acid ratio of [B]/[TEB] = 0.25/1.5 resulted in higher conversion compared to that of [B]/[TEB] = 0.25/0.5 but unexpectedly produced a lower $M_{n,GPC}$ (entries 8 and 9 in Table 1). These findings suggest that an excess of acid may promote side reactions during polymerization, potentially hindering the overall process. When DP of 150 was targeted, the monomer conversion markedly decreased to 24% due to the increased monomer-to-base ratio and the corresponding reduction in activity of the base (entry 10 in Table 1). To address this, the stronger phosphazene base *t*-BuP$_2$ (pK_a = 33.5 in MeCN) was used instead of *t*-BuP$_1$ (pK_a = 26.9 in MeCN),[23] which led to an increased conversion of 80% along with a higher molecular weight (entry 11 in Table 1). However, a low molecular weight fraction appeared in the GPC trace, attributed to the chain termination caused by the transfer of a proton from activated terminal alkyne (Figure S7). Overall, these results indicate that precise control is achieved for the polymerization up to DP of 100 ($Đ \approx 1.1$), and PGPEs up to DP of 200 can be accessed under optimized conditions; however, sensitivities to catalyst ratios and side reactions may lead to partial loss of control at higher targeted DPs (above 150).

To verify the potential chemical interactions between the alkyne moiety and catalysts during polymerization, we performed ^{1}H NMR analyses. Upon mixing the GPE monomer and TEB in an equimolar ratio, slight downfield shifts were observed in the ^{1}H NMR spectrum for protons adjacent to the triple bond, 0.0026 ppm for the propargylic proton and 0.0010 ppm for the terminal alkyne proton. Concurrently, comparable shifts were observed for protons near the ether oxygen atoms (Figure S8). Alongside the ^{1}H NMR results, corresponding downfield shifts were observed in the ^{13}C NMR spectra as well (Figure S9). These shifts suggest a decrease in electron density around the alkyne and ether moieties, indicating an interaction between the GPE monomer and TEB. This observation aligns with a previous study by Feng and co-workers,[24] who attributed a similar downfield shift of the allylic proton in allyl glycidyl ether to an interaction with TEB. In addition to these peak shifts, a substantial decrease was observed in the peak ratio of the terminal alkyne proton (2.47 ppm) relative to that of the propargylic proton (4.25 ppm) (Figure 2b). Notably, when an equimolar amount of *t*-BuP$_1$ was further introduced, the terminal alkyne proton signal diminished even further. This trend is attributed to the increased acidity of the

https://doi.org/10.1021/acsmacrolett.5c00486
ACS Macro Lett. 2025, 14, 1344−1351

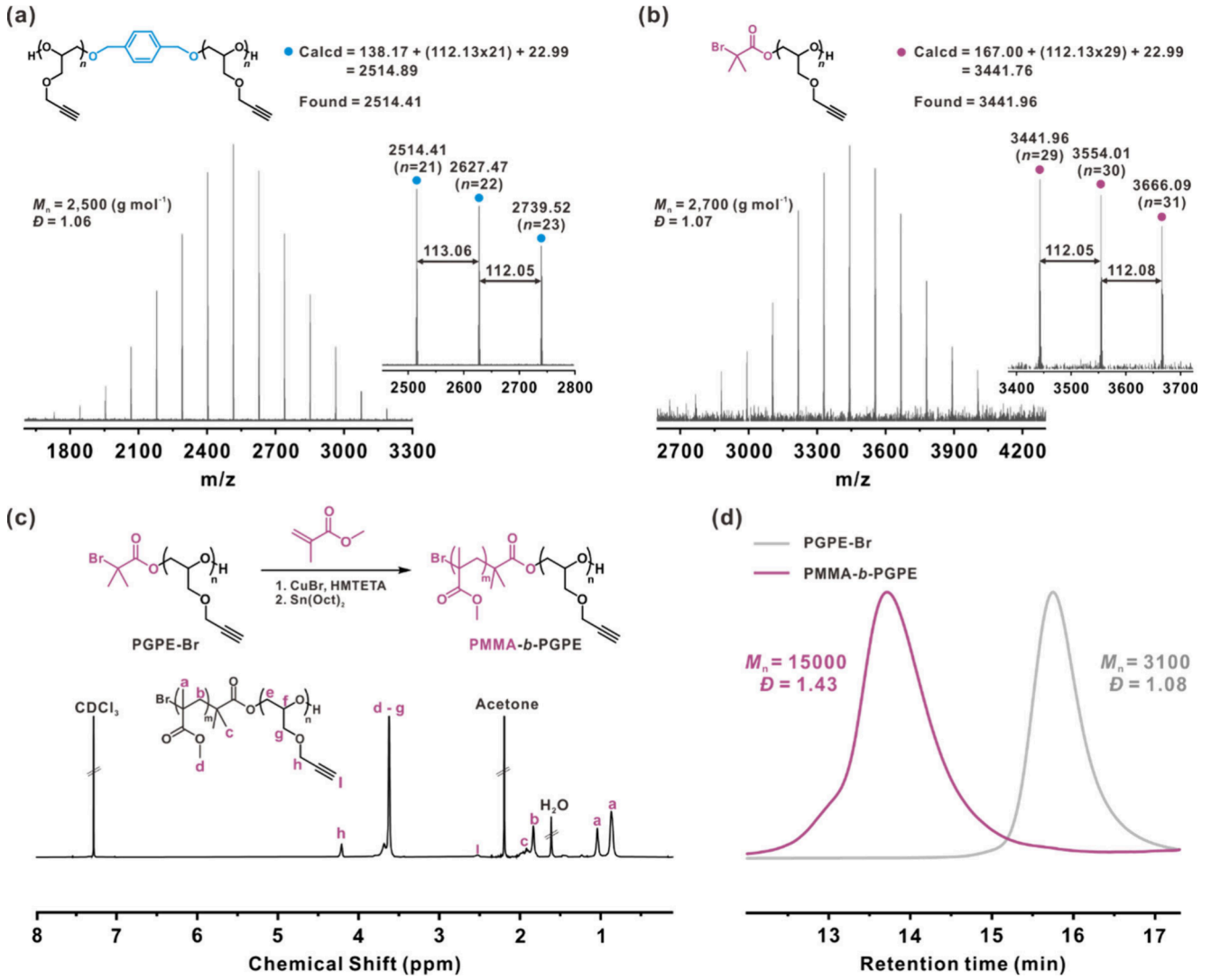

Figure 3. (a and b) Representative MALDI-TOF spectra of PGPE homopolymers initiated with (a) 1,4-benzenedimethanol and (b) 2-bromoisobutyric acid (see the Experimental Section for conditions), (c) ^{1}H NMR spectrum of $PMMA_{118}$-*b*-$PGPE_{30}$, and (d) GPC traces of $PGPE_{30}$–Br (gray) and $PMMA_{118}$-*b*-$PGPE_{30}$ (purple).

terminal alkyne proton upon complexation with TEB, rendering it more susceptible to deprotonation by the phosphazene base. A similar decrease was observed when GPE and *t*-BuP_1 were combined in a 1:1 molar ratio without TEB, suggesting proton exchange between the terminal alkyne and the base, even in the absence of a Lewis acid. Interestingly, this interaction was further evidenced in polymerization. For example, the ^{1}H NMR spectrum of the crude sample displayed a diminished terminal alkyne signal, which was restored following catalyst removal, indicating interactions between the monomer and Lewis pair catalyst during the reaction (Figure S10).

Collectively, these experimental results suggest that interactions between the catalysts (TEB and *t*-BuP_1) and the monomer influence the polymerization process (Scheme S1). Given the interaction between the terminal alkyne and TEB, increasing the acid-to-base ratio not only promotes the activation of the epoxide group but also facilitates the activation of the alkyne moiety. This dual activation promotes undesired early stage termination due to the increased acidity of terminal alkynes, resulting in a decrease of the number-average molecular weight despite higher monomer conversion. Meanwhile, increasing monomer-to-base ratios for targeting high DP leads to an accelerated termination rate, while the late-stage propagation rate is almost maintained, decreasing conversion and lowering molecular weight. Therefore, maintaining a consistent acid-to-base ratio is essential for achieving controlled polymerization in this study, particularly when targeting higher DP values.

To explore the scope of initiators for GPE polymerization using Lewis pair catalysts, additional polymerizations were conducted with benzyl alcohol, propargyl alcohol, and 2-bromoisobutyric acid as initiators (entries 1, 2, and 3 in Table S1). All reactions were performed in bulk, targeting a DP of 25. Notably, the GPC traces of the resulting PGPEs displayed monomodal peaks with low molecular dispersity ($Đ$ < 1.1), indicating well-controlled polymerization irrespective of the initiator type (Figure S10). To further assess the initiation efficiency, the absolute molecular weights of PGPEs were analyzed by matrix-assisted laser desorption/ionization time-of-flight (MALDI-TOF) mass spectrometry (Figure 3a and b and Figure S12). The MALDI-TOF spectra of the PGPEs exhibit a single distribution without any detectable secondary series, with a constant interval of 112.05 g mol^{-1} correspond-

https://doi.org/10.1021/acsmacrolett.5c00486
ACS Macro Lett. 2025, 14, 1344−1351

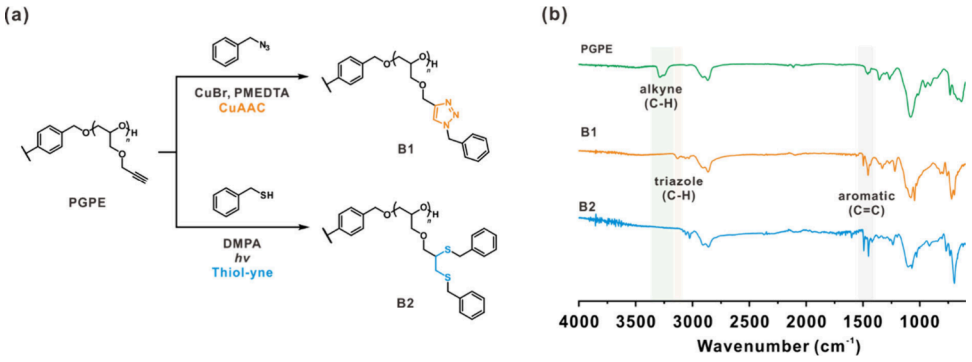

Figure 4. (a) Scheme for the post-polymerization modification of PGPE via CuAAC and thiol−yne reactions and (b) FTIR spectra of $PGPE_{50}$ (green), B1 (orange), and B2 (blue).

ing to the molar mass of a GPE repeating unit. Moreover, the absolute molecular weights corresponded to the calculated values based on the respective initiators employed. These results demonstrate that the Lewis pair catalyst system, comprising a phosphazene base and TEB, enables controlled polymerization with a wide range of initiators and high initiation efficiency (>99%). In particular, the successful polymerization using propargyl alcohol further confirms the compatibility of this system with terminal alkyne groups. This enables the straightforward one-step synthesis of alkyne-terminated polyethers, which could be useful for block copolymer synthesis or polymer topology control.

Furthermore, we confirmed that 2-bromoisobutyric acid can serve as an initiator under Lewis pair catalysis. This is consistent with prior reports, including those by Zhao and co-workers, showing that Lewis pair catalysis can accommodate carbonyl-bearing initiators by suppressing nucleophilic attack at carbonyl, thereby expanding the initiator scope.[25−27] Accordingly, PGPE with a bromo terminal group (i.e., $PGPE_{30}$−Br) was successfully synthesized and subsequently employed as a macroinitiator for ATRP to produce poly(methyl methacrylate)-*b*-poly(glycidyl propargyl ether) (PMMA-*b*-PGPE). Characteristic PMMA proton peaks were observed at 0.84, 1.01, 1.75−2.05, and 3.60 ppm in the ^{1}H NMR spectrum after polymerization (Figure 3c). Moreover, a shift toward a lower elution volume region in the GPC trace compared to PGPE−Br confirms the successful synthesis of the diblock copolymer (Figure 3d).

PGPE-based block copolymers were also achieved through the polymerization of GPE using a macroinitiator. In this process, PEO (M_n = 20 000 g/mol) was employed as the initiator and a combination of *t*-BuP_2 and TEB served as the catalyst system. Following the reaction, the GPC trace displayed a clear shift toward a lower elution volume compared to that for pristine PEO, indicating an increase in molecular weight due to the formation of terminal PGPE blocks (Figure S13a). Furthermore, the ^{1}H NMR spectrum of the purified product exhibited characteristic peaks at 2.48 and 4.18 ppm, corresponding to the acetylene proton and propargylic methylene protons, respectively, confirming the successful synthesis of the triblock copolymer PGPE-*b*-PEO-*b*-PGPE (Figure S13b). Such ABA-type triblock copolymers, comprising hydrophobic end blocks and a hydrophilic midblock, can form physically cross-linked hydrogels through the association of the end blocks upon hydration. For instance, synthesized PGPE-*b*-PEO-*b*-PGPE formed a slightly opaque hydrogel at a concentration of 3.0 wt % in deionized water, indicating successful network formation in aqueous media (Figure S14). This finding highlights the potential of the PGPE-based triblock copolymer as a functional soft material suitable for biomedical applications.

After confirmation of the feasibility of synthesizing various PGPE-based polymers, post-polymerization modification of PGPE was performed through two independent reactions, CuAAC and thiol−yne reactions, to demonstrate its chemical versatility (Figure 4a).

The FTIR spectra obtained after CuAAC revealed the disappearance of the terminal alkyne C−H stretch at 3300 cm^{-1}, along with the emergence of new bands near 3100 cm^{-1} and within the 1400−1500 cm^{-1} region, corresponding to the C−H stretch of the triazole ring and the C═C stretch of the benzene ring, respectively (Figure 4b). In the ^{1}H NMR spectrum, the characteristic proton signals of pristine PGPE, specifically the propargylic proton at 4.25 ppm and the terminal alkyne proton at 2.47 ppm, were no longer observed after the reaction (Figure S15). Additionally, new peaks corresponding to the triazole proton (7.55 ppm) and methylene protons adjacent to the triazole ring (4.49 and 5.41 ppm) appeared, further confirming the successful transformation of the terminal alkyne group into a benzyl group.

In addition, the thiol−yne reaction was performed using benzyl mercaptan and 2,2-dimethoxy-2-phenylacetophenone (DMPA) under UV irradiation at 365 nm. FTIR analysis confirmed the consumption of the pendant alkyne group and the introduction of the benzyl moiety (Figure 4b). In agreement with the CuAAC results, alkyne signals disappeared from the ^{1}H NMR spectrum, while a pronounced increase was observed in the aromatic proton signals at 7.2−7.4 ppm (Figure S15). The emergence of new peaks corresponding to thioether linkage at 3.1−3.4 ppm also confirmed the successful incorporation of the benzyl group via thiol−yne addition. Taken together, these findings validate that both CuAAC and thiol−yne reactions enable efficient and selective post-functionalization of alkyne-bearing polyethers, affording structurally distinct benzyl-modified polymers under orthogonal reaction conditions.

In summary, we achieved the controlled polymerization of GPE using Lewis pair organocatalysts, thereby overcoming the limitations of conventional anionic ROP, which is hindered by the acidity of terminal alkynes. Most importantly, interactions of the alkyne moiety with both the phosphazene base and Lewis acid necessitated precise control over the catalyst ratio to achieve higher DP values with narrow dispersity. The

https://doi.org/10.1021/acsmacrolett.5c00486
ACS Macro Lett. 2025, 14, 1344−1351

proposed system enabled efficient polymerization using various initiators, providing access to well-defined polymers with diverse chain-end functionalities. The resulting PGPEs served as versatile building blocks for advanced polymer architectures, including a PMMA-*b*-PGPE diblock copolymer synthesized via ATRP and a PGPE-*b*-PEO-*b*-PGPE triblock copolymer obtained through a macroinitiator strategy. Finally, the pendant alkyne groups allowed versatile post-polymerization modifications via CuAAC and thiol−yne reactions, underscoring the broad potential of alkyne-functionalized polyethers.

■ ASSOCIATED CONTENT

Supporting Information

The Supporting Information is available free of charge at https://pubs.acs.org/doi/10.1021/acsmacrolett.5c00486.

Experimental procedures and additional analyses, including ^{1}H, ^{13}C, COSY, and HSQC NMR, GPC, and MALDI-TOF (PDF)

■ AUTHOR INFORMATION

Corresponding Author

Byeong-Su Kim − *Department of Chemistry, Yonsei University, Seoul 03722, Republic of Korea;* orcid.org/0000-0002-6419-3054; Email: bskim19@yonsei.ac.kr

Authors

Byungwoo Yoo − *Department of Chemistry, Yonsei University, Seoul 03722, Republic of Korea*

Jinsu Baek − *Department of Chemistry, Yonsei University, Seoul 03722, Republic of Korea;* orcid.org/0000-0002-6393-9176

Complete contact information is available at: https://pubs.acs.org/10.1021/acsmacrolett.5c00486

Author Contributions

†Byungwoo Yoo and Jinsu Baek contributed equally to this work. CRediT: **Byungwoo Yoo** formal analysis, investigation, visualization, writing - original draft; **Jinsu Baek** formal analysis, investigation, validation, writing - original draft; **Byeong-Su Kim** investigation, project administration, supervision, writing - original draft, writing - review & editing.

Notes

The authors declare no competing financial interest.

■ ACKNOWLEDGMENTS

This work was supported by the National Research Foundation of Korea (RS-2025-00558644).

■ REFERENCES

(1) Banjare, S. K.; Mahulkar, P. S.; Nanda, T.; Pati, B. V.; Najiar, L. O.; Ravikumar, P. C. Diverse Reactivity of Alkynes in C−H Activation Reactions. *Chem. Commun.* **2022**, *58*, 10262−10289.

(2) Hosseininezhad, S.; Ramazani, A. Recent Advances in the Application of Alkynes in Multicomponent Reactions. *RSC Adv.* **2024**, *14*, 278−352.

(3) Zeng, H.; Zeng, P.; Baek, J.; Kim, B.-S.; Müllner, M. Self-Assembly of Amorphous 2d Polymer Nanodiscs with Tuneable Size, Ph-Responsive Degradation and Controlled Drug Release. *Angew. Chem., Int. Ed.* **2025**, *64*, No. e202424269.

(4) Chen, C.; Singh, M. K.; Wunderlich, K.; Harvey, S.; Whitfield, C. J.; Zhou, Z.; Wagner, M.; Landfester, K.; Lieberwirth, I.; Fytas, G.; et al. Polymer Cyclization for the Emergence of Hierarchical Nanostructures. *Nat. Commun.* **2021**, *12*, 3959.

(5) Isono, T.; Satoh, Y.; Miyachi, K.; Chen, Y.; Sato, S.-i.; Tajima, K.; Satoh, T.; Kakuchi, T. Synthesis of Linear, Cyclic, Figure-Eight-Shaped, and Tadpole-Shaped Amphiphilic Block Copolyethers via *t*-Bu-P_4-Catalyzed Ring-Opening Polymerization of Hydrophilic and Hydrophobic Glycidyl Ethers. *Macromolecules* **2014**, *47*, 2853−2863.

(6) Satoh, Y.; Matsuno, H.; Yamamoto, T.; Tajima, K.; Isono, T.; Satoh, T. Synthesis of Well-Defined Three- and Four-Armed Cage-Shaped Polymers via "Topological Conversion" from Trefoil- and Quatrefoil-Shaped Polymers. *Macromolecules* **2017**, *50*, 97−106.

(7) Krimalowski, A.; Thelakkat, M. Sequential Co-Click Reactions with Poly(Glycidyl Propargyl Ether) toward Single-Ion Conducting Electrolytes. *Macromolecules* **2019**, *52*, 4042−4051.

(8) Offenloch, J. T.; Mutlu, H.; Barner-Kowollik, C. Interrupted CuAAC Ligation: An Efficient Approach to Fluorescence Labeled Three-Armed Mikto Star Polymers. *Macromolecules* **2018**, *51*, 2682−2689.

(9) Johnson, J. A.; Lewis, D. R.; Díaz, D. D.; Finn, M. G.; Koberstein, J. T.; Turro, N. J. Synthesis of Degradable Model Networks via ATRP and Click Chemistry. *J. Am. Chem. Soc.* **2006**, *128*, 6564−6565.

(10) Macdougall, L. J.; Pérez-Madrigal, M. M.; Shaw, J. E.; Worch, J. C.; Sammon, C.; Richardson, S. M.; Dove, A. P. Using Stereochemistry to Control Mechanical Properties in Thiol-Yne Click-Hydrogels. *Angew. Chem., Int. Ed.* **2021**, *60*, 25856−25864.

(11) Long, N. J.; Williams, C. K. Metal Alkynyl Σ Complexes: Synthesis and Materials. *Angew. Chem., Int. Ed.* **2003**, *42*, 2586−2617.

(12) Herzberger, J.; Leibig, D.; Langhanki, J.; Moers, C.; Opatz, T.; Frey, H. "Clickable PEG" Via Anionic Copolymerization of Ethylene Oxide and Glycidyl Propargyl Ether. *Polym. Chem.* **2017**, *8*, 1882−1887.

(13) Chen, J.; Bhat, V.; Hawker, C. J. High-Throughput Synthesis, Purification, and Application of Alkyne-Functionalized Discrete Oligomers. *J. Am. Chem. Soc.* **2024**, *146*, 8650−8658.

(14) Carlotti, S.; Labbé, A.; Rejsek, V.; Doutaz, S.; Gervais, M.; Deffieux, A. Living/Controlled Anionic Polymerization and Copolymerization of Epichlorohydrin with Tetraoctylammonium Bromide−Triisobutylaluminum Initiating Systems. *Macromolecules* **2008**, *41*, 7058−7062.

(15) Jung, P.; Ziegler, A. D.; Blankenburg, J.; Frey, H. Glycidyl Tosylate: Polymerization of a "Non-Polymerizable" Monomer Permits Universal Post-Functionalization of Polyethers. *Angew. Chem., Int. Ed.* **2019**, *58*, 12883−12886.

(16) Herzberger, J.; Frey, H. Epicyanohydrin: Polymerization by Monomer Activation Gives Access to Nitrile-, Amino-, and Carboxyl-Functional Poly(Ethylene Glycol). *Macromolecules* **2015**, *48*, 8144−8153.

(17) Illy, N.; Fu, H.; Mongkhoun, E. Simple/Commercially Available Lewis Acid in Anionic Ring-Opening Polymerization: Powerful Compounds with Multiple Applications in Macromolecular Engineering. *ChemCatChem.* **2025**, *17*, No. e202401032.

(18) Ferrier, R. C.; Kumbhar, G.; Crum-Dacon, S.; Lynd, N. A. A Guide to Modern Methods for Poly(Thio)Ether Synthesis Using Earth-Abundant Metals. *Chem. Commun.* **2023**, *59*, 12390−12410.

(19) Kwon, G.; Kim, M.; Jung, W. H.; Park, S.; Tam, T.-T. H.; Oh, S.-H.; Choi, S.-H.; Ahn, D. J.; Lee, S.-H.; Kim, B.-S. Designing Cooperative Hydrogen Bonding in Polyethers with Carboxylic Acid Pendants. *Macromolecules* **2021**, *54*, 8478−8487.

(20) Chen, Y.; Shen, J.; Liu, S.; Zhao, J.; Wang, Y.; Zhang, G. High Efficiency Organic Lewis Pair Catalyst for Ring-Opening Polymerization of Epoxides with Chemoselectivity. *Macromolecules* **2018**, *51*, 8286−8297.

(21) Češarek, U.; Liu, L.; Chen, Q.; Wen, T.; Žagar, E.; Zhao, J.; Pahovnik, D. Acidity Reversal Enables Site-Specific Ring-Opening Polymerization of Epoxides from Biprotonic Compounds. *J. Am. Chem. Soc.* **2025**, *147*, 5189−5196.

(22) Pang, J.; Lai, T.; Zhao, J. Selective Ring-Opening Polymerization of Silyl Glycidyl Ether through Organocatalysis. *ACS Macro Lett.* **2024**, *13*, 859−865.

(23) Schwesinger, R.; Schlemper, H.; Hasenfratz, C.; Willaredt, J.; Dambacher, T.; Breuer, T.; Ottaway, C.; Fletschinger, M.; Boele, J.; Fritz, H.; et al. Extremely Strong, Uncharged Auxiliary Bases; Monomeric and Polymer-Supported Polyaminophosphazenes (P_2−P_5). *Liebigs Ann.* **1996**, *1996*, 1055−1081.
(24) Jia, M.; Zhang, D.; de Kort, G. W.; Wilsens, C. H. R. M.; Rastogi, S.; Hadjichristidis, N.; Gnanou, Y.; Feng, X. All-Polycarbonate Thermoplastic Elastomers Based on Triblock Copolymers Derived from Triethylborane-Mediated Sequential Copolymerization of CO_2 with Various Epoxides. *Macromolecules* **2020**, *53*, 5297−5307.
(25) Chen, Y.; Liu, S.; Zhao, J.; Pahovnik, D.; Žagar, E.; Zhang, G. Chemoselective Polymerization of Epoxides from Carboxylic Acids: Direct Access to Esterified Polyethers and Biodegradable Polyurethanes. *ACS Macro Lett.* **2019**, *8*, 1582−1587.
(26) Liu, L.; Zhao, J.; Zhang, G. Chemoselectivity Streamlines the Approach to Linear and Y-Shaped Thiol-Polyethers Starting from Thiocarboxylic Acids. *ACS Macro Lett.* **2023**, *12*, 1185−1192.
(27) Xia, Y.; Scheutz, G. M.; Easterling, C. P.; Zhao, J.; Sumerlin, B. S. Hybrid Block Copolymer Synthesis by Merging Photoiniferter and Organocatalytic Ring-Opening Polymerizations. *Angew. Chem., Int. Ed.* **2021**, *60*, 18537−18541.

https://doi.org/10.1021/acsmacrolett.5c00486
ACS Macro Lett. 2025, 14, 1344−1351